

# Gravo-aeroelastic scaling of very large wind turbines to wind tunnel size

H Canet<sup>1</sup>, P Bortolotti<sup>1</sup>, CL Bottasso<sup>1,2</sup>

<sup>1</sup> Wind Energy Institute, Technische Universität München, Garching, Germany

<sup>2</sup> Department of Aerospace Science and Technology, Politecnico di Milano, Milano, Italy

E-mail: [carlo.bottasso@tum.de](mailto:carlo.bottasso@tum.de)

**Abstract.** This work focuses on the design of wind turbine rotors of wind tunnel size that match the aerodynamic (for both rotor and wake) and aeroelastic behavior of multi-MW machines, including gravitational effects. The approach follows the classical definition of length, time and mass scaling ratios to respect nondimensional scaling parameters. The sub-scale model is obtained by a complete aero-structural re-design procedure, considering airfoils with similar polars at sub-scale Reynolds and the use of adequate materials. The approach is applied to the design of a sub-scale wind tunnel rotor that mimics the behavior of a 10 MW wind turbine. Results illustrate the main characteristics of the proposed method as well as its limitations, highlighting the challenges posed by representing a gravo-aeroelastic system at a much reduced scale.

## 1. Introduction

Significant research efforts are currently being devoted to the development of very large wind turbines. Motivated by the reduction in cost of energy, the size of rotors has indeed dramatically increased in the last decades, and it is expected to grow even more in the next generation of wind turbines. Nonetheless, the design of very large machines remains a challenging activity, especially because of the currently only limited understanding of the aeroelastic and gravitational effects on very flexible rotors and towers. In addition, there is a need for validated numerical models that are capable of simulating such complex systems with the necessary level of confidence. Indeed, high-quality full-scale experimental data is difficult, expensive and sometimes altogether impossible to obtain.

In this scenario, scaled models offer a viable mean to overcome these hurdles. Complementary to full-scale experiments, tests performed on scaled models can provide relevant experimental data, obtained in the controlled environment of a lab, capturing selected aspects of the behavior of the full-scale system. This can be achieved at costs that are orders of magnitude lower than the ones associated with full-scale field testing. In addition, some measurements are possible in a wind tunnel that are not achievable at full-scale with the same level of accuracy or in the same conditions. Of course, these advantages come at a price, as it is typically impossible to match exactly all physical processes that take place at full-scale using a scaled model. Therefore, scaled models have to be designed with specific goals in mind, and they will inevitably suffer from limitations.

Aeroelastic sub-scale models of wind tunnel size have been developed for years, but the scaling of gravitational effects has so far been typically neglected, as the enforcement of other



quantities was prioritized. However, the larger the rotors, the more prevalent the effects of gravity, which should therefore be included in the scaling procedures. This research work aims at closing this gap, proposing an aeroelastic scaling design methodology that includes gravitational effects. A modern automated multi-disciplinary design procedure is used to support and ease the implementation of the proposed scaling approach.

The paper is divided into three main sections. The first is devoted to the description of the theoretical background from which the scaling laws are derived. These conditions are then formulated as design drivers within an aero-structural design procedure, which is described in Sect. 2.2. In the last section, the described approach is applied to design a 2.8 meter sub-scale rotor reproducing the aerodynamic and dynamic behavior of a 10 MW offshore wind turbine.

## 2. Design methodology

### 2.1. Scaling laws

The starting point for the formulation of scaling laws lies on seven nondimensional numbers, which are obtained from the application of Buckingham II Theorem to the equations governing the dynamic behavior of wind turbines [1]. One can classify these quantities into two categories. The first corresponds to the numbers that can be simultaneously enforced in the sub-scale model. These include the tip-speed ratio (TSR, describing the kinematics of the rotor aerodynamics), the nondimensional time, the nondimensional natural frequencies (which determine the ratio of elastic to inertial forces, in relation to the rotor speed), and the Lock number (which sets the relation between aerodynamic and inertial forces). The second category includes instead quantities that cannot be simultaneously guaranteed in the sub-scale model, when testing in air in standard wind tunnels. These include the Reynolds number (representing the ratio of inertial to viscous forces), the Mach number (which describes the flow compressibility), and the Froude number (defined as the ratio of aerodynamic to gravitational forces). For modern very large machines, gravitational loads play an important role, and the correct representation of their effects requires the enforcement of the Froude number in the sub-scale model. This however typically generates a mismatch in the Reynolds and Mach numbers. While the latter may be neglected—at least for today’s typical tip speeds—the former is of much greater importance and leads to marked changes in the aerodynamic performance of the blades.

Enforcing these matching conditions allows for the derivation of the scaling ratios that define the sub-scale characteristics. The length scaling ratio  $\eta_l$  between sub-scale ( $R_s$ ) and full-scale ( $R_f$ ) rotor radius is defined as

$$\eta_l = \frac{R_s}{R_f}. \quad (1)$$

Enforcing the Froude number, one obtains the following relation between sub-scale ( $T_s$ ) and full-scale ( $T_f$ ) time:

$$\eta_t = \frac{T_s}{T_f} = \sqrt{\eta_l}. \quad (2)$$

Finally, the mass scaling ratio  $\eta_m$ , expressed as sub-scale mass ( $M_s$ ) over full-scale mass ( $M_f$ ), is obtained from the matching of the Lock number and writes

$$\eta_m = \frac{M_s}{M_f} = \eta_l^3. \quad (3)$$

An overview of these scaling conditions, as well as their implications in the definition of the time and mass scaling ratios, is given in Fig. 1.

Conditions simultaneously matched				Conditions simultaneously not matched		
Dynamic response	Kinematics	Aero/Inertia	Elastic/Inertia	Gravity	Inertia/Viscous	Compressibility
$\tau_s = \tau_f$	$TSR_s = TSR_f$	$Lo_s = Lo_f$	$\tilde{\omega}_s = \tilde{\omega}_f$	$Fr_s = Fr_f$	$Re_s \neq Re_f$	$Ma_s \neq Ma_f$
		$\eta_m = \eta_f^3$	$E_s = E_f \eta_t$	$\eta_t = \sqrt{\eta_l}$		

Figure 1: Scaling laws for very large wind turbines and their implications on the scaling ratios ( $E$  indicates Young modulus).

The simplest possible scaling strategy consists in a straightforward zooming-down of the full-scale machine, where all system characteristics are scaled according to the aforementioned scaling ratios [2]. When aiming at a wind tunnel model size, this approach is however typically difficult to implement. First, the effect of the Reynolds mismatch between the two scales would lead to very significant deviations in the aerodynamic performance of the airfoils. Furthermore, zooming down the structural characteristics would imply extremely thin components made of materials with peculiar and possibly unrealistic mechanical properties. Therefore, an alternative approach must be taken, based on a complete aero-structural re-design.

## 2.2. Aero-structural re-design

An aero-structural re-design approach is here proposed by formulating two separate optimization problems. Both are implemented in the wind turbine design tool **Cp-Max** [3, 4]. This code is wrapped around the high-fidelity aeroservoelastic multibody simulation model **Cp-Lambda** (Code for Performance, Loads, Aeroelasticity by Multi-Body Dynamic Analysis) [5], which performs the necessary aeroelastic calculations. The design tool is coupled to the 2D finite-element cross sectional code **ANBA**, which implements the theory of Giavotto et al. [6]. This tool provides the structural and inertial characteristics of each beam section, serving as input for the multibody model.

The optimization algorithms implemented within **Cp-Max** perform the complete design of a wind turbine, including its control laws. The present sub-scale design activity represents a special application of these general design procedures. In particular, the present case demands the sequential solution of the blade aerodynamic and structural optimization problems, as illustrated in Fig. 2. Both procedures employ a Sequential Quadratic Programming (SQP) optimization algorithm, in which gradients are computed by means of finite differences.

The first design problem focuses on the definition of a scaled shape that mimics the aerodynamic behavior of the full-scale system. This is obtained by ensuring a number of conditions. First, the two rotors should have the same TSR for optimal power coefficient. Second, they should have the same spanwise circulation distribution, which ensures the same shed vorticity in the wake. Third, the airfoils should have the same efficiencies. Unfortunately, this last requirement cannot be met in general, because of the very different sectional Reynolds numbers of the two rotors. To approximate this condition, the scaled rotor is equipped with airfoils that differ from the ones of the full-scale machine, but that have similar (or as similar as possible) polars at their lower operating Reynolds. Based on these requirements, the scaled rotor is designed by optimizing its maximum power coefficient at the desired TSR, while satisfying a target spanwise distribution of the circulation. The resulting shape will be in general quite different from the one of the full-scale rotor, but matches as well as possible its aerodynamic characteristics.

In the second optimization, given the aerodynamic shape defined in the first problem, the blade structure is re-designed to mimic the full-scale aeroelastic behavior, considering available materials and feasible geometries. The structural solution is obtained by designing a blade that

has the same placement of natural frequencies with respect to the rotor speed, as well as the same Lock number of the full-scale one.

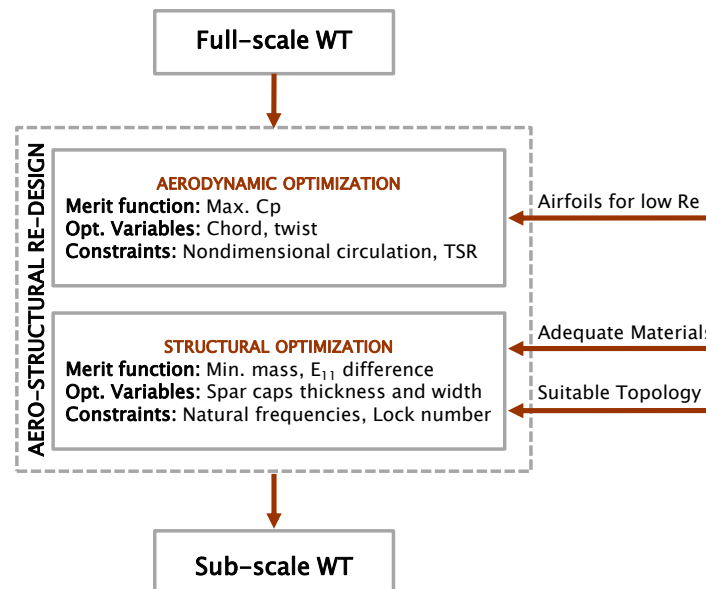


Figure 2: Overview of the proposed aero-structural re-design process.

The structural configuration of the scaled blade can be very different from the one of the full-scale machine. In the present work, we consider a solid blade—in contrast to the typical thin-walled structures used at full-scale—, made with a lightweight foamy material, two spar caps and a thin layer of glue that ensures a smooth finish to the surface. The modeling of the cross sections in ANBA is based on quadrilateral planar finite elements, where a meshing procedure implemented in Matlab guarantees simultaneously an accurate representation of the geometry and good aspect ratios for the elements. The geometry is parameterized in terms of spanwise shape functions and associated degrees of freedom. In turn, these structural parameters are computed by solving a design problem that minimizes the difference between the scaled and full-scale mass and flapwise stiffness distributions, while satisfying the frequency placement and Lock number constraints.

### 3. Scaling of a 10 MW rotor to wind tunnel size

The proposed scaling laws and design method are used to develop a sub-scale rotor of 2.8 meters based on the INNWIND.EU 10 MW wind turbine [7]. The length, time and mass scaling ratios for this problem are reported in Table 1, together with the scaling factors for other key quantities. The scaling of all system characteristics only depends on the ratio between the full- and the sub-scale rotor diameters. The re-designed sub-scale machine will have a different external shape and internal configuration, under the enforcement of the scaled parameters reported in Table 2. However, the matching of shape and configuration are irrelevant, as long as the significant scaling conditions are preserved between the two models.

Table 1: Scaling factors derived from the scaling laws.

Quantity	Scaling factor	
Length	$n_l$	1:63.68
Time	$\sqrt{n_l}$	1:7.98
Mass	$n_l^3$	1:258214
Rotor Speed	$\sqrt{n_l}$	1:7.98
Wind Speed	$\sqrt{n_l}$	1:7.98
Reynolds	$n_l^{3/2}$	1:508.16
Stiffness	$n_l^5$	1:32360

Table 2: Full-scale and sub-scale model characteristics.

Data	Full-scale	Sub-scale
Rotor diameter	178.3 m	2.8 m
Hub height	119 m	1.87 m
Total blade mass	42 t	0.165 kg
TSR for max $C_P$	7.2	7.2
Rotor speed	8.9 rpm	71.1 rpm
First flapwise frequency	0.57 Hz	4.52 Hz
First edgewise frequency	0.72 Hz	5.77 Hz

### 3.1. Aerodynamic re-design

The airfoil chosen for the aerodynamic re-design is the RG14 [8], whose shape is compared to the full-scale tip airfoil in Fig. 3a. This airfoil has already been successfully adopted in the context of the INNWIND.EU project [9] to design the rigid rotor of a floating wind turbine. The goal there was to represent the aerodynamic characteristics of the same 10 MW wind turbine considered here.

Although less efficient than the full-scale tip airfoil (Fig. 3a), the RG14 airfoil is found to approximate the polars of the full-scale blade sufficiently well at the low Reynolds generated in the wind tunnel, as shown in Fig. 3c and 3d. The airfoil is used from 20% blade span to the tip. The blade root cylinder smoothly deforms into the RG14 airfoil in the blade inner region, resulting in the relative thickness distribution shown in Fig. 4b.

The blade chord and twist distributions are optimized to reproduce the aerodynamic performance of the full-scale machine as closely as possible. A comparison between the initial and the re-designed blade shapes and nondimensional spanwise circulation distributions are reported in Fig. 4. The enforcement of circulation matching—which is quite good except at 0.22% span—is the active driver for the outer blade shape. In terms of performance, the re-designed blade can only approximate the full-scale one, mostly because of the unavoidable differences in the airfoil behavior at the much reduced Reynolds number.

### 3.2. Structural re-design

The structural re-design of the blade starts from the work of Campagnolo et al. [10], where an aeroelastically scaled blade for wind tunnel testing was designed and manufactured. For that blade, the time scaling ratio was not driven by the enforcement of the Froude number, but it was based on a trade-off between Reynolds mismatch and an excessive control bandwidth. This implied a lower time scaling ratio than the present one, which in turn led to a significantly stiffer blade. In addition, the blade was designed to mirror the full-scale aeroelastic behavior, by achieving a realistic distribution of the inertial and stiffness properties, as well as ensuring the

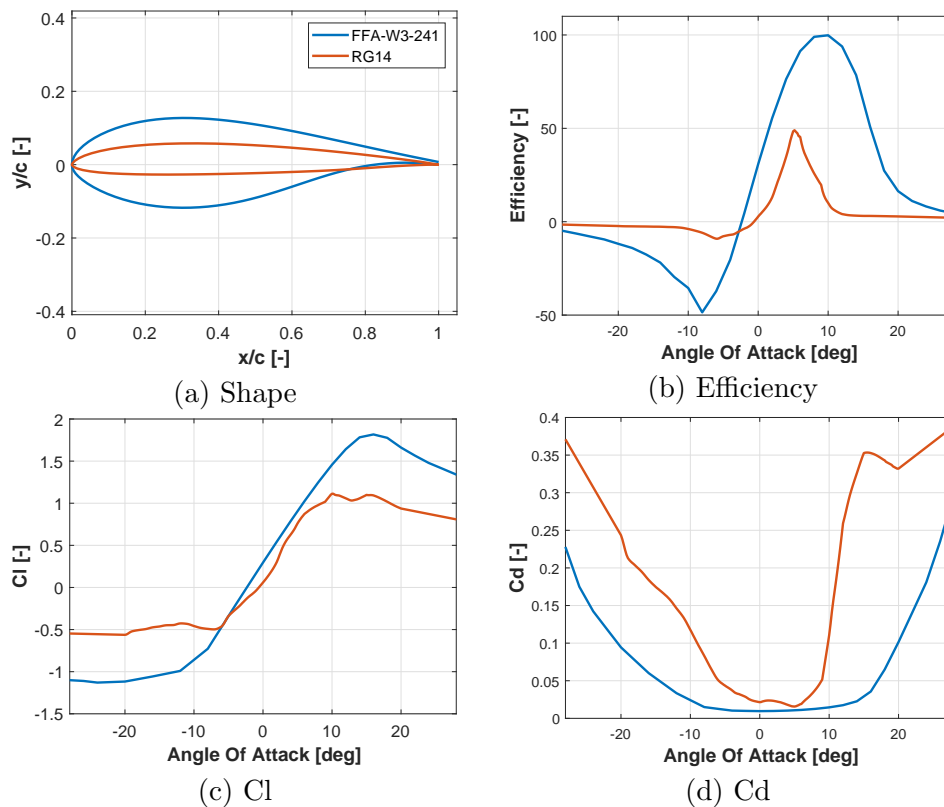


Figure 3: Comparison of aerodynamic characteristics for the full-scale model tip airfoil FFA-W3-241 ( $Re=1E7$ ) and the low-Reynolds airfoil RG14 ( $Re=5E4$ ).

same placement of natural frequencies with respect to the rotor speed between the two models. The blade structure adopted a solid sectional layout filled with a foam core made of Rohacell, which was machined to provide the outer blade shape. Two unidirectional carbon spar caps provided the required flapwise stiffness distribution. The surface smoothness was obtained by a very thin layer of skin made of glue. The blade re-design was able to replicate the placement of the lowest four rotor natural frequencies and it approximated the mass and flapwise stiffness distributions, but it was stiffer than the full-scale reference in the edgewise direction.

Despite the differences in scaling laws, and thus in desired aeroelastic behavior, the layout developed in Ref. [10] was found to be a suitable solution even in the present case. The selection of materials is a critical aspect of the problem, and the mechanical properties listed in the Cambridge University Materials Data Book [11] are used to guide the material selection process for spar caps and core. A Rigid Polymer Foam (LD) [11] is chosen as filler, because of its relatively high stiffness and lightness. For the spar caps, thermoplastic polymers are found to be the most suitable family of materials. Even though their stiffness to density ratio is much lower than materials traditionally used for spar caps, such as CFRP, they are well suited to this application. Moreover, the use of thermoplastics allows for alternative and easier manufacturing methods, leading to a higher flexibility in the spar cap design. From this family, polypropylene (PP) is chosen because of its low stiffness modulus. Finally, the external shell is covered by a very thin layer of the epoxy structural adhesive Scotch Weld AF 32 [12].

The structural design procedure implemented in Cp-Max [4] and described in Sect. 2.2 is then used to optimize the spar caps thickness and width and ensure the matching of all desired scaling constraints. The problem formulation also includes manufacturability constraints for

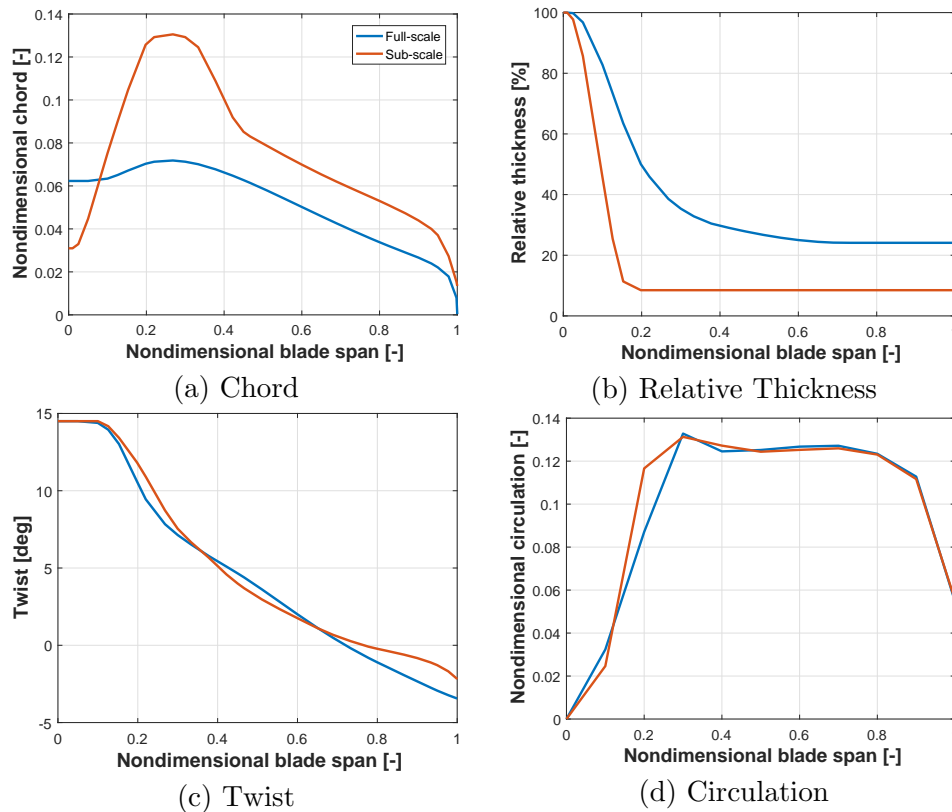


Figure 4: Comparisons of external shape and nondimensional circulation in Region 2, for the full- and the sub-scale models.

the components, establishing a 1 mm minimum thickness of the spar caps. The constraint satisfaction tolerance is set at 5%. Figure 5 reports the results of the optimization. The desired matching of mass and flapwise stiffness is achieved, except at blade root. The requirement on edgewise stiffness is instead not met due to the large chord of the sub-scale model. The placement of the first flapwise and edgewise frequencies with respect to the rotor speed is also successfully achieved. However, the corrected placement of higher frequencies is not exactly met. Finally, small disparities in mass distribution introduce a slight mismatch in the Lock number.

#### 4. Conclusions

This work has proposed an approach to develop sub-scale models of wind tunnel size to mimic the gravo-aeroelastic behavior of large wind turbines. The formulation was applied to the design of a 2.8 meter sub-scale model of a 10 MW machine.

The aero-structural re-design approach is able to obtain the desired results, although subject to limitations. Specifically, the replication of the power coefficient vs. TSR behavior is limited by the availability of suitable low-Reynolds airfoils. Furthermore, the structural re-design is constrained by the manufacturing process and by the mechanical properties of existing materials. As a result, only a partial matching of the inertial and elastic behavior can be achieved. More precisely, flapwise stiffness and mass distributions are well matched from 20% of blade span to blade tip, resulting in the correct placement of the lowest two natural frequencies of the blade. These results highlight the challenges posed by representing a gravo-aeroelastic system at a much reduced scale. Although it is clear that the resulting scaled model is unable to exactly replicate the one at full scale, several relevant physical processes are nonetheless well

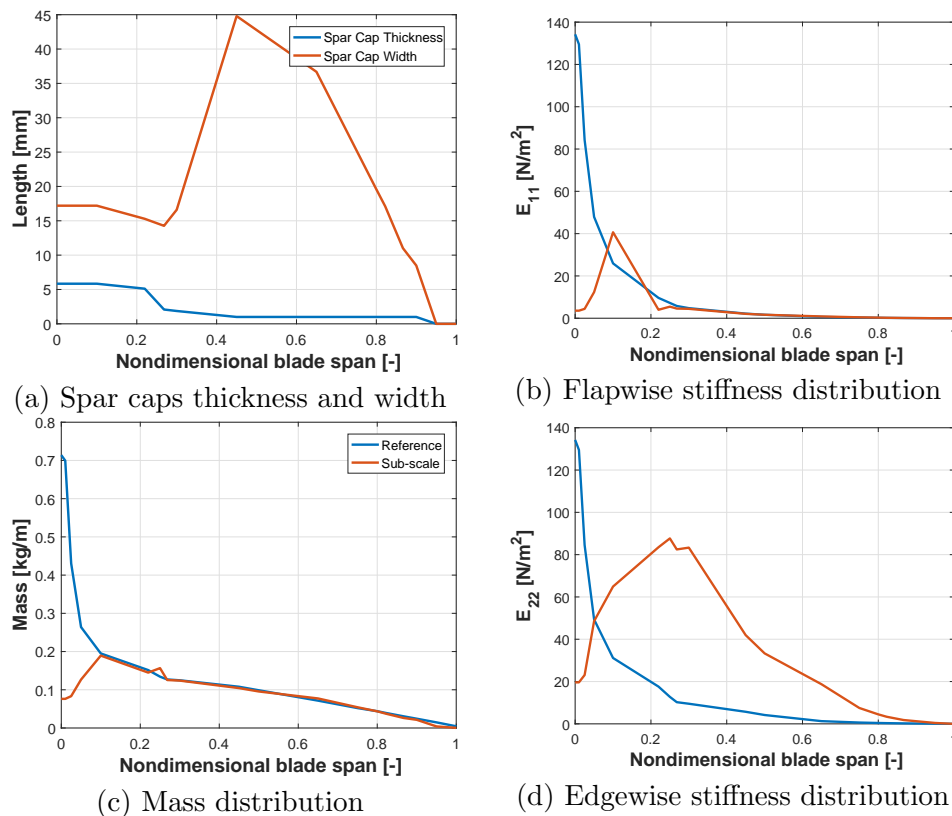


Figure 5: Distribution of spar cap thickness and width along blade span, and comparison between the cross sectional properties of the sub-scale and scaled full-scale model.

represented at the smaller scale. Keeping always well in mind the limits of scaled models, wind tunnel experiments can still play a crucial role in the validation and verification of simulation models, in the understanding of the physics, in the testing of control laws, the exploration of new configurations, and many other relevant activities.

The present research will continue by further investigating the blade structural design, looking in particular at the manufacturing process and the corresponding design limits. Moreover, efforts will be devoted to improve the scaled model edgewise behavior, either by identifying materials with more suitable mechanical properties, or relaxing the aerodynamic constraints.

### Acknowledgments

The authors wish to thank Dr. Filippo Campagnolo for providing an initial rigid model of the 1.4 m blade, as well as airfoil polars for low Reynolds numbers.

### References

- [1] Bottasso CL, Campagnolo F and Petrovic V 2014 Wind tunnel testing of scaled wind turbine models: beyond aerodynamics *J. Wind Eng. Ind. Aerodyn.* **127** 1128 doi: 10.1016/j.jweia.2014.01.009
- [2] Loth E, Fingersh L, Griffith D, Kaminski M and Qin C 2017 Gravo-Aeroelastically Scaling for Extreme-Scale Wind Turbines *35th AIAA Applied Aerodynamics Conference*, AIAA AVIATION Forum, doi: 10.2514/6.2017-4215
- [3] Bottasso CL, Campagnolo F and Croce A 2012 Multi-disciplinary constrained optimization of wind turbines *Multibody Syst. Dyn.* **27** 21-53 doi: 10.1007/s11044-011-9271-x
- [4] Bortolotti P, Bottasso CL and Croce A 2016 Combined preliminary-detailed design of wind turbines *Wind Energ. Sci.*, **1** 71-88 doi: 10.5194/wes-1-71-2016



- [5] Bottasso CL, Croce A, Savini B, Sirchi W and Trainelli L 2006 Aero-servo-elastic modeling and control of wind turbines using finite-element multibody procedures 2006 *Multibody Syst. Dyn.* **16** 291-308 doi: 10.1007/s11044-006-9027-1
- [6] Giavotto V, Borri M, Mantegazza P and Ghiringhelli G 1983 Anisotropic beam theory and applications *Comput. Struct.* **16** 403-13 10.1016/0045-7949(83)90179-7
- [7] Bottasso CL, Bortolotti P, Croce A and Gualdoni F 2016 Integrated aero-structural optimization of wind turbines *Multibody Syst. Dyn.* **38** 317-44 doi: 10.1007/s11044-015-9488-1
- [8] Selig M, Guglielmo J, Broeren A and Gigure P 1995 *Summary of Low-Speed Airfoil Data* (Virginia: SoarTech Publications)
- [9] INNWIND.EU Deliverable 4.24. Results of wave tank tests.
- [10] Campagnolo F, Bottasso CL and Bettini P 2014 Design, manufacturing and characterization of aero-elastically scaled wind turbine blades for testing active and passive load alleviation techniques within a ABL wind tunnel *J. Phys.:Conf. Ser.* **524** 012061 doi: 10.1088/1742-6596/524/1/012061
- [11] Cambridge University Engineering Department 2003 Materials Data Book
- [12] Scotch-Weld: Structural Adhesive Film AF 32. Technical Data, Issue No. 3 doi: <https://multimedia.3m.com/mws/media/241415O/3mtm-scotch-weldtm-structural-adhesive-film-af-32.pdf>